Advances in Science and Technology Research Journal

Advances in Science and Technology Research Journal 2024, 18(5), 19–31
https://doi.org/10.12913/22998624/189512
ISSN 2299-8624, License CC-BY 4.0

Received: 2024.05.14
Accepted: 2024.06.26
Published: 2024.08.01

Application of Recurrence Quantification Analysis in the Detection of Osteoarthritis of the Knee with the Use of Vibroarthrography

Anna Machrowska[1], Robert Karpiński[1*], Marcin Maciejewski[2], Józef Jonak[1], Przemysław Krakowski[3,4], Arkadiusz Syta[2]

[1] Department of Machine Design and Mechatronics, Faculty of Mechanical Engineering, Lublin University of Technology, ul. Nadbystrzycka 36, 20-618 Lublin, Poland

[2] Department of Electronics and Information Technology, Faculty of Electrical Engineering and Computer Science, Lublin University of Technology, ul. Nadbystrzycka 36, 20-618 Lublin, Poland

[3] Department of Trauma Surgery and Emergency Medicine, Medical University of Lublin, ul. Staszica 11, 20-081 Lublin, Poland

[4] Orthopaedic and Sports Traumatology Department, Carolina Medical Center, ul. Pory 78, 02-757, Warsaw, Poland

* Corresponding author's e-mail: r.karpinski@pollub.pl

ABSTRACT

Nowadays, the world is struggling with the problems of an aging society. With the increasing share of older people in the population, degenerative joint diseases are a growing problem. The result of progressive degenerative changes in joints is primarily the deterioration of the patients' quality of life and their gradual exclusion from activity and social life. The ability to effectively, non-invasively and quickly detect cases of chondromalacia of the knee joints is a challenge for modern medicine. The possibility of early detection of progressive degenerative changes allows for the appropriate selection of treatment protocols and significantly increases the chances of inhibiting the development of degenerative diseases of the musculoskeletal system. The article presents a non-invasive method for detecting degenerative changes in the knee joints based on recurrence analysis and classification using neural networks. The result of the analyses was a classification accuracy of 91.07% in the case of multilayer perceptron (MPL) neural networks and 80.36% for radial basis function (RBF) networks.

Keywords: knee joint, cartilage, lubrication, wear, osteoarthritis, RBF, MLP.

INTRODUCTION

Osteoarthritis is debilitating condition in which hyaline cartilage degenerates. As the disease progresses, the mechanical parameters of the articular cartilage change, and thus the friction and lubrication parameters in the biological bed that is the knee joint. As a result, loss of joint motion, pain and stiffness occur, which leads to disability [1]. Around the globe over 527 million individuals suffer from osteoarthritis (OA) [2, 3], what is even more concerning is that the disease can be found in younger population of patients [4, 5]. The problem with OA is that this is an ongoing process in which multiple tissues become rearranged in an irreversible way. Nevertheless, the first tissue breakdown is apparent in cartilage. During OA mechanical and tribological properties of cartilage change dramatically [6–8], decreasing the ability to produce smooth and painless motion in the affected joint. Cartilage has very limited healing capacity [9] and once injured, further breakdown is to be expected. With progression of the disease, impairment of daily activities – including work and leisure – becomes, apart from pain, the main disease burden for the affected individuals. In clinical setting, only accurate and fast diagnosis at early disease stages

can enable treatment, which will prolong joint survivor time. At the moment, the mainstay in OA diagnosing is conventional radiography, which is based on grading system proposed by Kellgren and Lawrence [10]. However, this imaging modality shows only reactive bone response to cartilage damage; therefore, diagnosis of cartilage lesion is delayed by nature. Magnetic resonance imaging (MRI), which at the moment is the most accurate imaging modality for cartilage lesion detection, has its drawbacks such as long examination time, need for skilled and trained staff as well as cost efficiency and long awaiting time [11]. MRI referrals should be given to the individuals with high suspicion of cartilage damage; however, up to 25% of patients referred for knee MRI have not received a proper orthopaedic examination prior to MRI [12]. As a result, this prolongs the awaiting time for the patient with high necessity for accurate joint evaluation. Moreover, due to the demand of accessibility of the MRI, less experienced radiologists evaluate the images and image acquisition is performed on lower quality equipment, and this in result was shown in the conducted studies to grossly underestimate the cartilage lesion grade of cartilage lesion [13]. Therefore, orthopaedic community seeks a diagnostic modality, which would be fast, cheap, reproducible, automated and reliable in both orthopaedic and general practitioners setting. As it was mentioned above, OA changes mechanical and tribological properties of cartilage, which as a result changes acoustic emission of the joint. On the basis of this information, it can be assumed that changes in cartilage parameters and thus osteoarthritis can be identified based on typical methods used in vibroacoustic diagnostics of machinery. In the case of machinery, vibroacoustic diagnostics is a method of assessing the condition of equipment by analyzing vibrations and acoustic emissions [14, 15]. With this technique, it is possible to detect early signs of damage, allowing a faster response and minimizing repair costs. Vibroacoustic analysis is particularly useful in monitoring the condition of bearings, gears, motors and other mechanical components, enabling precise location and assessment of wear or damage. Therefore, in literature vibroarthrography (VAG) has been proposed as a cartilage lesion detection method. Joint auscultation was firstly introduced in 1902 [16]; however, little research have been conducted on this topic for almost a century. Vibroacoustic signals recorded for knee joints are nonlinear and nonstationary. Nonlinearity arises from complex interactions within the joint, which are difficult to describe using linear models. Nonstationarity means that the statistical properties of these signals, such as mean and variance, change over time depending on the type and intensity of movement. Consequently, advanced methods suitable for analyzing nonlinear and time-varying signals are used for their analysis.

Recurrence quantitative analysis (RQA) is a method of nonlinear analysis of biomedical signals that is used in diagnostics and health monitoring [17–19]. It is employed in cardiology to analyze heart rate variability, in neurology to examine EEG signals, in pulmonology to assess respiratory functions, and in rehabilitation to monitor movement [20, 21]. RQA is particularly effective at identifying subtle changes in signals, which facilitates early detection of disorders and supports the development of personalized medicine.

In recent years, multiple papers showing possible clinical application of VAG have been published [22–26]. Authors' previous studies have proven that VAG can be a reliable method of cartilage lesion detection with diagnostic accuracy surpassing 90% in the knee joint [27–30]. In these papers, authors' diagnostic system as well as acquisition and signal processing methods were described in detail. However, in literature up to this date there is no consensus regarding the best practice in VAG acquisition and processing; therefore, in this study the authors aimed to investigate recurrence quantification as a potential processing method for further development of VAG systems.

MATERIALS AND METHODS

Group characteristics and recording of vibroacoustic signals

The study included a group of 112 volunteers, 63 of whom were healthy subjects, while 49 were orthopedic outpatients with pre-confirmed osteoarthritis of the knee qualified for surgery. Qualification for treatment was carried out by a licensed orthopedic surgeon based on typical physical tests to assess damage to anatomical structures within the knee joint and imaging studies such as MRI and radiography (X-ray). The basis for the analyses carried out were acoustic signals collected during tests conducted on a group of volunteers in the conditions of the orthopedic department,

as well as in the laboratories of the Lublin University of Technology. The study received a positive opinion from the Bioethics Committee of the Medical University of Lublin, approval number KE-0254/261/2019.

Within the framework of cooperation between Lublin University of Technology and the Independent Public Health Care Center in Łęczna and the Medical University of Lublin, an experimental study was carried out, during which the data used in the article were collected. As the primary source of information, bench tests conducted with the use of the measurement system developed by the authors, implemented under the conditions of the orthopedic department and laboratory rooms of the Lublin University of Technology, were adopted.

The measurement system was based on an Arduino Mega2560 R3 module. Three CM01B [31] piezoelectric contact microphones connected to analog inputs were used for signal acquisition. These microphones were then attached with double-sided adhesive tape at three anatomical locations, that is, on the condyles of the femur on the lateral and medial sides and on the patella. A galvanic barrier was used on the USB connector to ensure patient safety, and the device itself was powered by an 11.1V lithium-ion battery. Measurement of the limb position angle was carried out using an EMS22A50-D28-LT6 Bourns encoder, built into the pivot axis of a typical Breg T-Scope Knee orthosis. The block diagram of the adopted system is presented in Figure 1. In addition, a detailed description of the solution is presented in papers [32–34]. Vibroacoustic signals were recorded for repetitive sequences of knee joint straightening and bending movements in the range of 90°–0°–90°. The study was performed for sequences performed in an open kinetic chain (OKC) [35, 36]. An OKC is a combination of sequentially arranged joints that constitute a complex motor unit, in which the end segments are free to move in space [37]. An example of such a chain would be knee extension in a sitting position. During the recording of signals in the open kinetic chain, the procedure was carried out in a loose overhang of the legs in the sitting position with the knees flexed at 90°, followed by full knee extension from 90° to 0° and flexion again (from 0° to 90°). Signals were recorded for 10 full repetitions of the described procedure.

Recurrence quantification analysis

As the degenerative disease progresses, the mechanical parameters of the articular cartilage change, and as a result, the friction and lubrication parameters in the joint change. The occurrence of osteoarthritis causes pain and limits movement. It can therefore be concluded that the vibroarthrorrhagic signals recorded for the patients diagnosed with chondromalacia of the knee joints will have different dynamics and structure than those recorded for the people from the control group. However, it should be noted that each of these waveforms has non-linear characteristics. The adopted signal analysis method has proven to be highly effective in identifying changes in the dynamics of nonlinear experimental systems based on short and noisy vibroacoustic time series [38–40]. From the point of view of

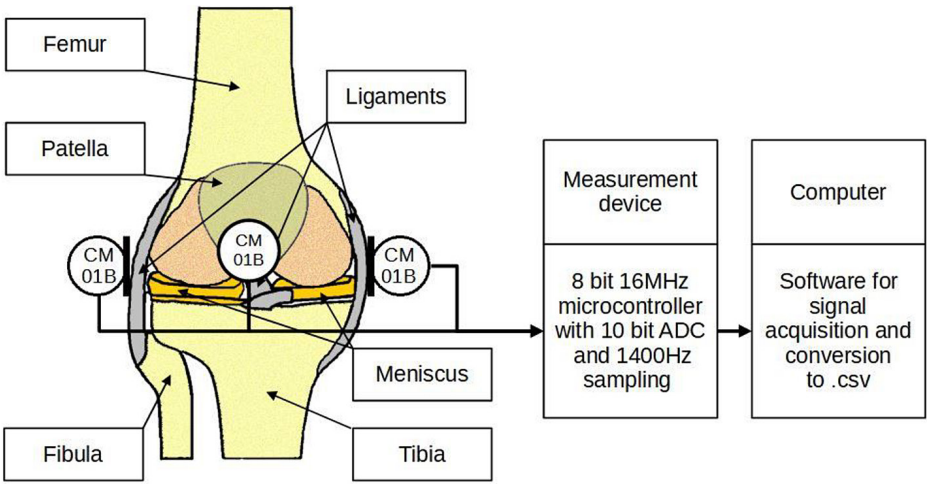

Figure 1. Block diagram of the measurement system

classifying the condition of knee joints, the use of recurrence analysis in the research was beneficial.

The first stage of this nonlinear analysis was the phase reconstruction process. In order to realize the reconstruction, the embedding properties must be tested. This is related to the properties of the phase space, which can be reconstructed by filling in the missing coordinates with time-delayed coordinates [41]. Describing the VAG input signal as V, sampled at time t with increment i can be written:

$$V_i = \left[V_i, V_{i-\Delta i}, V_{i-2\Delta i}, \ldots, V_{i-(M-1)\Delta i}\right] \quad (1)$$

where: Δi is the time delay and M is the embedding dimension. By researching *AMI* (average mutual information) [42, 43] and FNNF (False Nearest Neighbour Fraction) [42, 43] their values were obtained. *AMI* is described as the conditional probability of a sequence of events:

$$AMI(\delta_i) = -\sum_{kl} p_{kl}(\delta_i) ln \frac{p_{kl}(\delta_i)}{p_k p_l} \quad (2)$$

where: to divide the value into 116 equal parts, the amplitudes of the recorded acoustic signals fall within the range $V \in [V\text{min}, V\text{max}]$, p_k means the probability of finding the value of V in the kth interval and p_{kl} denotes the probability that V falls into the lth time interval δ_i. Optimal time delay $\Delta_i = \delta_i$ is determined on the basis of obtaining the first minimum of *AMI*, for which the investigated events are so independent that a new coordinate can be determined.

To obtain FNNF, the point indicated by V_i is selected and then the distance to nearest neighbor V_j is calculated in m- dimensional space. Through subsequent iterations, the parameter $Q_{i,m}$ is calculated and described as:

$$Q_{i,m} = \frac{|V_i - V_j|_{m+1}}{|V_i - V_j|_m} \quad (3)$$

The obtained Q_{im} value is compared with the selected Q_c threshold, and then the cases for which Q_{im} exceeds the indicated threshold value are calculated. The *FNNF* estimation is described as:

$$FNNF(m) = \frac{1}{N} \sum_i \Theta(Q_{i,m} - Q_c) \quad (4)$$

where: N is the number of waveform elements and $\Theta(x)$ is Heaviside step function. The fraction analysis is repeated until the optimal value $M = m$ is reached. Then, this means that some of the false neighbors tend to zero.

The result of the research for VAG signals in the control group were: $\Delta_i = 8$ and $M = 3$. These results allowed for further steps to be taken, such as determining parameters in the RQA analysis and comparing the results of the group of patients with osteoarthritis with the results in the control group. The recurrence plots are a method of visualizing matrices.

$$R_{i,j} = \Theta\left(\varepsilon_i - \left|x_i - x_j\right|\right) \quad (5)$$

where: $x_i \in R^d$; ε_i means the threshold value and i, $j = 1, 2, \ldots, N$. In the case of the current analysis, for the threshold value $\mathscr{E} = 0.56$ sample charts were obtained and presented in Figure 2 and Figure 3.

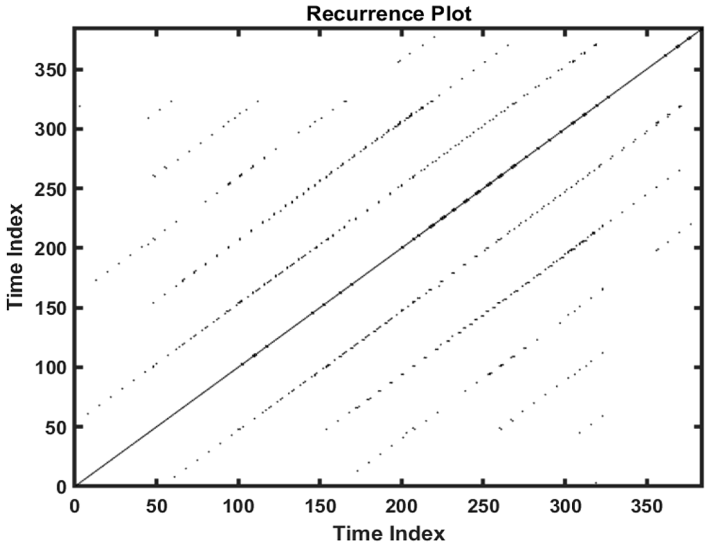

Figure 2. Recurrence plot of a person from the control group

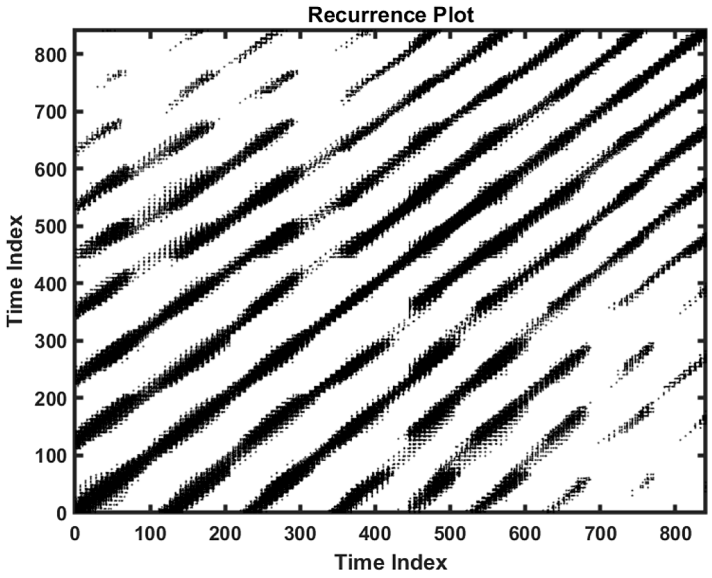

Figure 3. Recurrence plot of a person with diagnosed chondromalacia of knee joint

In further analyses, the VAG acoustic signals were qualitatively analyzed and recurrence indicators were determined, such as: recurrence rate (RR), determinism (DET), maximum length (LMAX), entropy (ENT), laminarity (LAM) and trapping time (TT). The *RR* parameter in qualitative analysis is defined as:

$$RR = \frac{1}{N^2}\sum_{i,j=1}^{N} R(i,j) \tag{6}$$

The recurrence rate determines the share of black dots on the RP graph, i.e. the density of repetition points. This coefficient corresponds to the probability of a specific condition reoccurring and similarity to previous system response. Another parameter used in further analyzes was determinism. It is defined as:

$$DET = \frac{\sum_{l=lmin}^{N} lP(l)}{\sum_{l=1}^{N} lP(l)} \tag{7}$$

where: $P(l)$ is the frequency distribution of length l diagonal lines. This measure is related to the predictability of the dynamic system. In comparison, white noise or nonperiodic behavior have an RP graph with single dots and very few diagonal lines, while a periodic process has an RP graph with a small number of single dots and long diagonal lines.

The next indicator examined was the largest length of the diagonal line LMAX. Another parameter analyzed was Shannon entropy, defined as follows:

$$ENT = -\sum_{l=l_{min}}^{N} p(l)\ln p(l) \tag{8}$$

Entropy reflects the degree of complexity of the deterministic structure of a system. Another indicator examined was laminarity. Laminarity is defined as:

$$LAM = \frac{\sum_{v=v_{min}}^{N} vP(v)}{\sum_{v=1}^{N} vP(v)} \tag{9}$$

where: $P(v)$ is the frequency distribution of the length v of vertical lines, starting from v_{min}. This measure is related to the number of laminar phases in the system (degree of intermittency).

The last of the examined indicators was trapping time (*TT*), described as:

$$TT = \frac{\sum_{v=v_{min}}^{N} vP(v)}{\sum_{v=v_{min}}^{N} P(v)} \tag{10}$$

It provides the information about the laminarity time, i.e. the time the system remains in a given state. The parameters presented above were used to classify the condition of the knee joints using neural networks.

Classification and evaluation of classifiers

The application of classification using neural networks in solving medical problems has opened up new possibilities in the diagnosis, monitoring and prognosis of the course of many diseases. Neural networks, with their ability to model complex patterns and relationships in large data sets, have become a key tool in precision medicine [44, 45]. In this study, multilayer perceptron and radial basis

function (RBF) radial basis function neural networks were used to solve the classification problem. Classification included case assignment to distinguish between healthy individuals (HC) and those with knee osteoarthritis (OA).

Multilayer perceptron neural networks are supervised learning networks with full inter-layer connectivity that consist of an input layer, one or more hidden layers, and an output layer. They use activation functions to model complex nonlinear relationships and learn using a back propagation algorithm, adjusting the connection weights. MLP is effective in pattern recognition, classification and prediction, finding applications in various fields such as medicine, finance, robotics and process control [46, 47].

RBF (radial basis function) neural networks are a type of neural networks characterized by the use of radial functions (e.g. Gaussian) in the hidden layer, which respond to the distance of the input vector from a fixed center. They consist of three layers: input, hidden layer with radial functions and output. Their main advantage is the ability to efficiently model complex spatial and nonlinear relationships. RBF networks are used in a wide range of applications, such as function approximation, classification, regression, and in control systems and forecasting, due to their speed and efficiency in interpolation in multidimensional data spaces [48, 49].

All calculations were carried out in the Statistica 13.3 software environment. The measures determined in the RQA analysis described in previous chapters were used as classifier inputs. They were determined separately for each anatomical location. A total of 18 parameters were adopted. Various subdivisions of data into training, validation, and testing sets, including 50–25–25 and 60–20–20, were evaluated. The results are presented for the subdivision where the data were randomly allocated as 70% for training, 15% for testing, and 15% for validation.

The comparison of classifiers was based on several key metrics, such as classification accuracy, which represents the ratio of correct predictions to the total number of observations. This measure can be misleading for unbalanced data. ROC and AUC curves were also used, given that they allow an assessment of the model's ability to distinguish between classes, with AUC as an overall measure of effectiveness. Due to the disparity of the analyzed groups, Matthews Correlation Coefficient and F1 Score values were determined. The Matthews correlation coefficient (MCC) takes into account all aspects of the confusion matrix, offering a balanced score for unbalanced sets [50]. The F1 score, on the other hand, is a harmonious average of precision and sensitivity, ideal for balancing both for unbalanced data [51]. It is important to tailor the choice of metrics to the specifics of the data and the problem, avoiding basing model evaluation on a single metric, and this is what was done in this paper.

RESULTS

This chapter presents the results of a multilayer perceptron and radial basis function neural network classification performed based on recurrence quantification analysis (RQA) values determined for acoustic signals generated by moving knee joints. Classification involved assigning cases to one of two groups, i.e. OA – subjects with confirmed degenerative changes, and HC – healthy volunteers without knee joint changes. All classification calculations were carried out in the Statistica version 13.3 software environment, which not only provided advanced data processing and neural network analysis tools, but also enabled detailed model verification and validation. Table 1 shows the detailed results of learning, testing and validation accuracy for each of the neural networks analyzed. The accuracy measure used varied depending on the type of output variable. For qualitative variables used in classification, accuracy was expressed as the relative number of correctly classified cases to the total number of cases.

In the learning group, a higher accuracy of 95% was obtained for the MPL network, while in the case of classification using the RBF network, the accuracy was 83.5%. The accuracy in the test set was 75% of correctly assigned cases for MPL and 62.5% for RBF, respectively. In the validation set, it was 87.5% of correctly assigned cases for MPL and 81.25% for RBF, respectively. The learning algorithm for MPL was BFGS 26, while for the RBF network it was RBFT. The BFGS (Broyden-Fletcher-Goldfarb-Shanno) algorithm is a popular quasi-Newtonian method used for numerical optimization to find local minima of differentiable functions. Rather than computing the Hesse matrix directly, the algorithm uses its approximation with an inverse that is updated at each iteration based on gradients. BFGS is

Table 1. Accuracy parameters for learning, testing and validation of the MLP and RBF neural network

Network name	Accuracy of learning	Accuracy of testing	Accuracy of validation	Learning algorithm	Error function	Activation (hidden)	Activation (output)
MLP 18-54-2	95.00	75.00	87.50	BFGS 26	SOS	Tanh	Linear
RBF 18-35-2	83.75	62.50	81.25	RBFT	Entropy	Gauss	Softmax

valued for its good convergence and efficiency, but its use can be limited for very large optimization problems due to the need to store matrices of large size. The error functions were SOS (sum of squares) for MLP and Entropy for RBF, respectively. For SOS, the error is calculated as the sum of the squares of the differences between the target values and the values obtained at the output of the individual output neurons. This is the typical error function used when training neural networks. In the case of Entropy, the error is the sum of the products of the set values and the logarithms of the errors for each output neuron. The activation function is the function used to transform the activation level of a unit (neuron) into an output signal. For MLP classification, the activation function was Tanh, while for RBF it was Gauss. The tanh (hyperbolic tangent) activation function transforms inputs to a range of -1 to 1 and is often used in the hidden layers of neural networks due to its centering and symmetry properties. Tanh helps maintain the scale of the data, which facilitates learning, but can lead to fading gradients, especially with large input values, which slows down the learning process. The function is also more computationally expensive than some other activation functions, such as ReLU. The Gaussian activation function is a less common, but interesting function used in neural networks. Instead of the traditional linear or nonlinear approach used by most activation functions, the Gaussian function is based on a normal distribution. The activation functions in the output layer were a linear function in MLP and – in the case of RBF Softmax – an exponential function, the value of which, however, is further normalized so that the sum of activations for the entire layer equals 1. The confusion matrix and details of the classification process for each method are shown in Table 2.

A higher classification accuracy 91.07% was achieved using MLP-type neural networks with 95.24% in the HC group and 85.71% in the OA group, respectively. For classification using RBF networks, the overall accuracy was almost 10% lower at 80.36% obtaining 85.71% correct assignments in the HC group and 73.47% in the OA group, respectively.

A summary of the ROC curves for each classification method is shown in Figure 4, while the parameters of the curves are presented in Table 3, along with other parameters that allow comparison of the selected classification methods.

Higher parameters were obtained with the MLP multilayer perceptron classifier for which the global accuracy was 91.07% with F1 score and MCC values of 0.894 and 0.819, respectively. The value of the area under the curve for this classification method was AUC = 0.943 with a sensitivity of 0.933 and specificity of 0.896.

For RBF, these parameters were lower. Global classification accuracy was just over 80% with F1 Score values of 0.804 and MCC values of 0.655.

Table 2. Confusion matrix and details of the classification process

Network name		HC	OA	Total
MLP 18-54-2	Total	63	49	112
	Correct	60	42	102
	Incorrect	3	7	10
	Correct (%)	95.24	85.71	91.07
	Incorrect (%)	4.76	14.29	8.93
RBF 18-35-2	Total	63	49	112
	Correct	54	36	90
	Incorrect	9	13	22
	Correct (%)	85.71	73.47	80.36
	Incorrect (%)	14.29	26.53	19.64

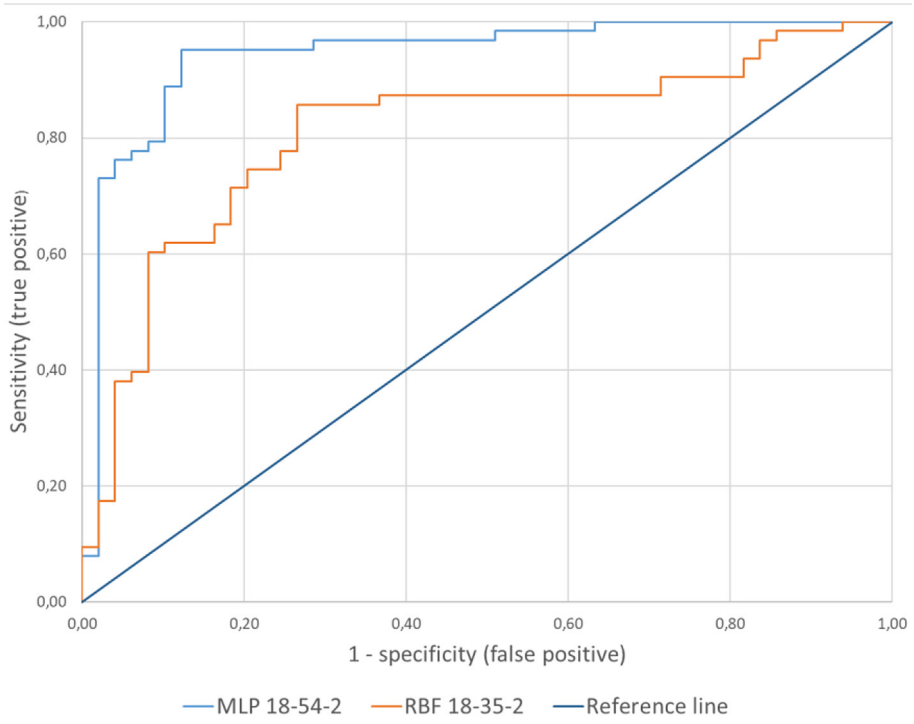

Figure 4. Comparison of ROC curves for all classification methods

The value of the area under the ROC curve for RBF was 0.766 with sensitivity and specificity of 0.800 and 0.806, respectively. Detailed parameters of the classifiers are shown in Table 3.

DISCUSSION

Vibroacoustic joint diagnostics combined with the use of neural network classification is a cutting-edge approach that combines advanced acoustic signal recording and processing techniques with machine learning to assess the health of knee joints. By analyzing the sounds produced by joints as they move, it is possible to pick up subtle anomalies that may indicate the early stages of osteoarthritis or other joint damage.

The method is based on the recording of the sounds and vibrations generated by the knee joint during the performance of standard repetitive motion sequences according to an established test protocol. The resulting recordings are then processed using specialized dedicated algorithms for analyzing nonlinear and non-stationary signals, which isolate their characteristic features. These features are later used as input for neural networks that have been trained to classify various joint conditions based on the previously collected data. The application of neural network-based classification in medicine is not without its challenges, such as ensuring data privacy and security, the interpretability of models, and the need for large datasets for training.

Nonetheless, the potential of this technology to contribute to advances in diagnosis and treatment is enormous, and its development and implementation are constantly being monitored and developed by the scientific and medical community. Up to date, there has been no strict protocol of acquisition and signal processing in regard to VAG. Factors such as sensor placement, examination protocol can affect significantly obtained results [52]. Also, the examination protocol including closed or open kinematic chain can affect the results [35]. Therefore, multiple factors can

Table 3. Details of classification parameters using the various methods

Network name	Accuracy (%)	Sensitivity	Specificity	AUC	ROC threshold	Precision	Recall	F1 score	MCC
MLP 18-11-2	91.07	0.933	0.896	0.943	0.631	0.857	0.933	0.894	0.819
RBF 18-29-2	80.36	0.800	0.806	0.809	0.544	0.735	0.800	0.766	0.599

influence the obtained results. In the conducted study, the authors have tried to answer the question concerning best signal processing method. Recurrence quantitative analysis which is utilized in analyzing other medical signals, especially in regard to subtle changes in recorded signals. In this study, a combination of RQA and MLP showed high specificity of 0.896 and high sensitivity of 0.933. These results correspond with other authors showing VAG to surpass 90% in sensitivity and specificity, as well as accuracy. Kieselev et al. [23] in their study showed similar sensitivity (0.92) but much lower specificity (0.78); however, their study was performed on small sample group (n = 28). Higher accuracy, reaching 0.94, was found in a study conducted by Nalband et al. In this study, least square support vector machines signal processing was introduced. However, this study was also performed on small sample (n = 24) [53]. Other approaches towards signal processing have also been published. On the basis of entropy analysis, the same research group showed accuracy reaching 0.86 [54]. On the other hand, Wu et al. showed that analysis of entropy can produce diagnostic accuracy oscillating at 0.8 [55]. Other research groups published their results showing 100% accuracy [26]. Table 4 summarizes the results presented by other authors in the literature.

However, most of these studies are subjected to a bias due to verification method, which is MRI. Even though MRI is gold standard in cartilage evaluation. it still underestimates the cartilage lesion grade and is more accurate in grade III and IV lesions rather than I and II [13]. Regardless of the lack of unified examination protocol, first clinical applications of VAG can be found in literature [66], which shows high potential for this diagnostic modality. However, further unification of results and finding the best method of acquisition and signal processing have to follow in order to fully use potential of VAG. Vibroacoustic diagnosis of the knee joint has numerous limitations that affect its effectiveness and clinical acceptance. Although it is less invasive and potentially faster, it does not provide as detailed information about the structure of the joint as MRI or CT. It requires additional studies to establish its reliability, reproducibility and standards of use. Interpretation of the results due to the complex processing of nonlinear and non-stationary VAG signals can be complicated, limiting its availability and use in daily clinical practice. In addition, its wide acceptance in the medical community is hampered by a lack of evidence for its effectiveness in a variety of diagnostic applications and a lack of well-defined testing protocols. The main limitations of the proposed method observed at the stage of the conducted research, undoubtedly include the size and diversity of the groups. Vibroacoustic joint diagnostics is evolving, offering future prospects, such as improved accuracy with modern sensors and algorithms, and integration with other diagnostic methods.

It has the potential for early detection and monitoring of degenerative diseases, which could reduce the costs and increase the availability of diagnostics, especially in less-resourced regions. In order to fully evaluate the analyzed problem and realize the potential of the proposed method, further studies should be carried out on a much larger number of cases, taking into account the

Table 4. Comparison diagnostic results of proposed method with other related works

Authors	Classification methods	Accuracy (%)	Sensitivity	Specificity	AUC
Mascarenhas et al. [56]	Random forest	80.89	0.868	0.765	0.817
Sharma and Acharya [57]	LS-SVM	89.89	0.914	0.889	N/A
Nalband et al. [58]	LS-SVM	83.14	0.981	0.622	0.671
Wu et al. [59]	Bayesian decision rule	86.67	0.750	0.936	0.910
Cai et al. [60]	Multi-classifier combination system	88.76	0.737	1.000	0.952
Karpiński [29]	MLP	90.00	0.917	0.885	0.941
Mu et al. [61]	Strict 2-surface proximal classifier	91.01	0.947	0.882	0.950
Zheng et al. [62]	SVM, Bayesian decision rule	91.76	0.884	0.952	0.912
Kim et al. [63]	Back-propagation neural network	95.40	0.920	0.987	N/A
Karpiński et al. [28]	MLP, RBF	98.53	0.958	1.000	1.000
Balajee et al. [64]	LS-SVM	98.67	0.934	0.937	N/A
Rangayyan and Wu [65]	RBF	98.89	0.921	0.882	0.917

full 4 – point scale according to the ICRS classification and determining the precise anatomical locations of the occurrence of degenerative changes. Additionally, future studies should focus on the angular position of the joint and conduct analyses across a broader range of motion, encompassing the full range of the knee joint. It will be informative to correlate the contact zone area with the recorded vibroacoustic signals. By understanding the contact area as a function of joint angle and analyzing the signal characteristics to assess the degree of damage, it will be possible to accurately localize degenerative changes. Efforts are also planned for standardization and wider clinical acceptance, supported by extensive research and collaboration between engineers and physicians.

CONCLUSIONS

Knee joint vibroacoustics is an innovative, non-invasive diagnostic method that assesses joint health by analysing the sounds and vibrations generated during movement. This technique can provide a quick and potentially less expensive alternative to traditional imaging methods such as MRI or CT. While it offers prospects for early diagnosis of joint disease, it requires further research to confirm its accuracy and reliability. Vibroacoustics has potential for use in disease monitoring and preventive screening. The results showed that the MLP-type neural network performed significantly better in solving the classification problem, obtaining a classification accuracy close to 91%. In conclusion, vibroacoustic diagnosis of knee joints using neural networks presents itself as a promising tool that could revolutionize the way joint health is diagnosed and monitored by offering a fast, accurate and non-invasive method of examination.

REFERENCES

1. Cui A, Li H, Wang D, Zhong J, Chen Y, Lu H. Global, regional prevalence, incidence and risk factors of knee osteoarthritis in population-based studies. E Clinical Medicine. 2020 Dec; 29–30: 100587.
2. Quicke JG, Conaghan PG, Corp N, Peat G. Osteoarthritis year in review 2021: epidemiology & therapy. Osteoarthritis and Cartilage. 2022 Feb; 30(2): 196–206.
3. Long H, Liu Q, Yin H, Wang K, Diao N, Zhang Y, Lin J., Guo A. Prevalence trends of site-specific osteoarthritis from 1990 to 2019: Findings From the Global Burden of Disease Study 2019. Arthritis & Rheumatology. 2022 Jul; 74(7): 1172–83.
4. Roemer F, Jarraya M, Niu J, Silva J, Frobell R, Guemrazi A. Increased risk for radiographic osteoarthritis features in young active athletes: a cross-sectional matched case–control study. Osteoarthritis and Cartilage. 2015 Feb; 23(2): 239–43.
5. Cameron K, Hsiao M, Owens B, Burks R, Svoboda SJ. Incidence of physician-diagnosed osteoarthritis amongactive duty United States military service members. Arthritis & Rheumatology. 2011 Oct; 63(10): 2974–82.
6. Grushko G, Schneiderman R, Maroudas A. Some biochemical and biophysical parameters for the study of the pathogenesis of osteoarthritis: a Comparison Between the Processes of Ageing and Degeneration in Human Hip Cartilage. Connective Tissue Research. 1989 Jan; 19(2–4): 149–76.
7. Moore AC, Burris DL. Tribological and material properties for cartilage of and throughout the bovine stifle: support for the altered joint kinematics hypothesis of osteoarthritis. Osteoarthritis and Cartilage. 2015 Jan; 23(1): 161–9.
8. Link JM, Salinas EY, Hu JC, Athanasiou KA. The tribology of cartilage: Mechanisms, experimental techniques, and relevance to translational tissue engineering. Clinical Biomechanics. 2020 Oct; 79: 104880.
9. Cibere J, Sayre EC, Guermazi A, Nicolaou S, Kopec JA, Esdaile JM, Thorne A., Singer J., Wong H. Natural history of cartilage damage and osteoarthritis progression on magnetic resonance imaging in a population-based cohort with knee pain. Osteoarthritis and Cartilage. 2011 Jun; 19(6): 683–8.
10. Kellgren JH, Lawrence JS. Radiological assessment of osteo-arthrosis. Ann Rheum Dis. 1957 Dec; 16(4): 494–502.
11. Krakowski P, Karpiński R, Maciejewski R, Jonak J. Evaluation of the diagnostic accuracy of MRI in detection of knee cartilage lesions using Receiver Operating Characteristic curves. J Phys: Conf Ser. 2021 Jan; 1736: 012028.
12. Solivetti FM, Guerrisi A, Salducca N, Desiderio F, Graceffa D, Capodieci G, Romeo P., Sperduti I., Canitano S. Appropriateness of knee MRI prescriptions: clinical, economic and technical issues. La radiologia medica. 2016 Apr; 121(4): 315–22.
13. Krakowski P, Karpiński R, Jojczuk M, Nogalska A, Jonak J. Knee MRI Underestimates the Grade of Cartilage Lesions. Applied Sciences. 2021 Feb 9; 11(4): 1552.
14. Figlus T, Kozioł M, Kuczyński Ł. The effect of selected operational factors on the vibroactivity of

upper gearbox housings made of composite materials. Sensors. 2019 Sep 29; 19(19): 4240.

15. Figlus T, Szafraniec P, Skrúcaný T. Methods of measuring and processing signals during tests of the exposure of a motorcycle driver to vibration and noise. IJERPH. 2019 Aug 28; 16(17): 3145.
16. Blodgett WE. Auscultation of the knee joint. The Boston Medical and Surgical Journal. 1902 Jan 16; 146(3): 63–6.
17. Shabani H, Mikaili M, Noori SMR. Assessment of recurrence quantification analysis (RQA) of EEG for development of a novel drowsiness detection system. Biomed Eng Lett. 2016 Aug; 6(3): 196–204.
18. Zhao K, Wen H, Guo Y, Scano A, Zhang Z. Feasibility of recurrence quantification analysis (RQA) in quantifying dynamical coordination among muscles. Biomedical Signal Processing and Control. 2023 Jan; 79: 104042.
19. Jonak K, Syta A, Karakuła-Juchnowicz H, Krukow P. The clinical application of EEG-signals recurrence analysis as a measure of functional connectivity: Comparative case study of patients with various neuropsychiatric disorders. Brain Sciences. 2020 Jun 16; 10(6): 380.
20. Gruszczyńska I, Mosdorf R, Sobaniec P, Żochowska-Sobaniec M, Borowska M. Epilepsy identification based on EEG signal using RQA method. Advances in Medical Sciences. 2019 Mar; 64(1): 58–64.
21. Yuan C, Zhu X., Liu G., Lei M. Classification of the surface EMG signal using RQA based representations. In: 2008 IEEE International Joint Conference on Neural Networks (IEEE World Congress on Computational Intelligence) [Internet]. Hong Kong, China: IEEE; 2008 [cited 2024 Apr 12]. 2106–11. Available from: http://ieeexplore.ieee.org/document/4634087/
22. Mascaro B, Prior J, Shark LK, Selfe J, Cole P, Goodacre J. Exploratory study of a non-invasive method based on acoustic emission for assessing the dynamic integrity of knee joints. Medical Engineering & Physics. 2009 Oct; 31(8): 1013–22.
23. Kiselev J, Ziegler B, Schwalbe HJ, Franke RP, Wolf U. Detection of osteoarthritis using acoustic emission analysis. Medical Engineering & Physics. 2019 Mar; 65: 57–60.
24. Shark LK, Chen H, Goodacre J. Knee acoustic emission: A potential biomarker for quantitative assessment of joint ageing and degeneration. Medical Engineering & Physics. 2011 Jun; 33(5): 534–45.
25. Bączkowicz D, Kręcisz K, Borysiuk Z. Analysis of patellofemoral arthrokinematic motion quality in open and closed kinetic chains using vibroarthrography. BMC Musculoskelet Disord. 2019 Dec; 20(1): 48.
26. Rangayyan RM, Oloumi F, Wu Y, Cai S. Fractal analysis of knee-joint vibroarthrographic signals via power spectral analysis. Biomedical Signal Processing and Control. 2013 Jan; 8(1): 23–9.
27. Karpiński R, Krakowski P, Jonak J, Machrowska A, Maciejewski M, Nogalski A. Diagnostics of Articular Cartilage Damage Based on Generated Acoustic Signals Using ANN—Part I: Femoral-Tibial Joint. Sensors. 2022 Mar 10; 22(6): 2176.
28. Karpiński R, Krakowski P, Jonak J, Machrowska A, Maciejewski M, Nogalski A. Diagnostics of Articular Cartilage Damage Based on Generated Acoustic Signals Using ANN—Part II: Patellofemoral Joint. Sensors. 2022 May 15; 22(10): 3765.
29. Karpiński R. Knee joint osteoarthritis diagnosis based on selected acoustic signal discriminants using machine learning. Applied Computer Science. 2022; 18(2): 71–85.
30. Jonak J, Karpinski R, Machrowska A, Krakowski P, Maciejewski M. A preliminary study on the use of EEMD-RQA algorithms in the detection of degenerative changes in knee joints. IOP Conf Ser: Mater Sci Eng. 2019 Dec 1; 710(1): 012037.
31. Contact microphone CM-01B, Technical Data Sheet. 2015; 3.
32. Karpiński R, Krakowski P, Jonak J, Machrowska A, Maciejewski M. Comparison of selected classification methods based on machine learning as a diagnostic tool for knee joint cartilage damage based on generated vibroacoustic processes. Appl Comput Sci. 2023 Dec 31; 19(4): 136–50.
33. Karpiński R, Krakowski P, Jonak J, Machrowska A, Maciejewski M, Nogalski A. Estimation of differences in selected indices of vibroacoustic signals between healthy and osteoarthritic patellofemoral joints as a potential non-invasive diagnostic tool. J Phys: Conf Ser. 2021 Dec 1; 2130(1): 012009.
34. Karpiński R, Krakowski P, Jonak J, Machrowska A, Maciejewski M, Nogalski A. Analysis of differences in vibroacoustic signals between healthy and osteoarthritic knees using EMD algorithm and statistical analysis. J Phys: Conf Ser. 2021 Dec 1; 2130(1): 012010.
35. Karpiński R, Machrowska A, Maciejewski M. Application of acoustic signal processing methods in detecting differences between open and closed kinematic chain movement for the knee joint. Applied Computer Science. 2019 Mar 31; 15(1): 36–48.
36. Machrowska A, Karpiński R, Krakowski P, Jonak J. Diagnostic factors for opened and closed kinematic chain of vibroarthrography signals. Applied Computer Science [Internet]. 2019 [cited 2020 Dec 20]; 15(3). Available from: http://yadda.icm.edu.pl/baztech/element/bwmeta1.element.baztech-9da426cc-646e-4a3e-8797-d4f57c125596
37. Ellenbecker TS, Davies GJ. Closed kinetic chain exercise: a comprehensive guide to multiple joint

exercise. Human Kinetics; 2001.

38. Litak G, Syta A, Gajewski J, Jonak J. Detecting and identifying non-stationary courses in the ripping head power consumption by recurrence plots. Meccanica. 2010 Aug; 45(4): 603–8.
39. Syta A, Czarnigowski J, Jakliński P. Detection of cylinder misfire in an aircraft engine using linear and non-linear signal analysis. Measurement. 2021 Apr; 174: 108982.
40. Koszewnik A, Ambroziak L, Ołdziej D, Dzienis P, Ambrożkiewicz B, Syta A, et al. Nonlinear recurrence analysis of piezo sensor placement for unmanned aerial vehicle motor failure diagnosis. Sci Rep. 2024 Apr 9; 14(1): 8289.
41. Takens F. Detecting strange attractors in turbulence. In: Rand D, Young LS, editors. Dynamical Systems and Turbulence, Warwick 1980 [Internet]. Berlin, Heidelberg: Springer Berlin Heidelberg; 1981 [cited 2024 May 7]. 366–81. (Lecture Notes in Mathematics; 898). Available from: http://link.springer.com/10.1007/BFb0091924
42. Chen Y, Yang H. Multiscale recurrence analysis of long-term nonlinear and nonstationary time series. Chaos, Solitons & Fractals. 2012 Jul; 45(7): 978–87.
43. Hui Y. Multiscale Recurrence Quantification Analysis of Spatial Cardiac Vectorcardiogram Signals. IEEE Trans Biomed Eng. 2011 Feb; 58(2): 339–47.
44. Machrowska A, Karpiński R, Jonak J, Szabelski J, Krakowski P. Numerical prediction of the component-ratio-dependent compressive strength of bone cement. Applied Computer Science. 2020 Sep 30; 16(3): 87–101.
45. Machrowska A, Szabelski J, Karpiński R, Krakowski P, Jonak J, Jonak K. Use of deep learning networks and statistical modeling to predict changes in mechanical parameters of contaminated bone cements. Materials. 2020 Nov 28; 13(23): 5419.
46. Gardner MW, Dorling SR. Artificial neural networks (the multilayer perceptron) – a review of applications in the atmospheric sciences. Atmospheric environment. 1998; 32(14–15): 2627–36.
47. Falkowicz K, Kulisz M. Prediction of buckling behaviour of composite plate element using artificial neural networks. Adv Sci Technol Res J. 2024 Feb 1; 18(1): 231–43.
48. Elanayar SVT., Shin YC. Radial basis function neural network for approximation and estimation of nonlinear stochastic dynamic systems. IEEE Trans Neural Netw. 1994 Jul; 5(4): 594–603.
49. Montazer GA, Giveki D, Karami M, Rastegar H. Radial basis function neural networks: A review. Computer Reviews Journal. 2018; 1(1): 52–74.
50. Chicco D, Jurman G. The advantages of the Matthews correlation coefficient (MCC) over F1 score and accuracy in binary classification evaluation. BMC Genomics. 2020 Dec; 21(1): 6.
51. Goutte C, Gaussier E. A Probabilistic Interpretation of Precision, Recall and F-Score, with Implication for Evaluation. In: Losada DE, Fernández-Luna JM, editors. Advances in Information Retrieval [Internet]. Berlin, Heidelberg: Springer Berlin Heidelberg; 2005 [cited 2024 May 2]. 345–59. (Hutchison D, Kanade T, Kittler J, Kleinberg JM, Mattern F, Mitchell JC, et al., editors. Lecture Notes in Computer Science; 3408). Available from: http://link.springer.com/10.1007/978-3-540-31865-1_25.
52. Madeleine P, Andersen RE, Larsen JB, Arendt-Nielsen L, Samani A. Wireless multichannel vibroarthrographic recordings for the assessment of knee osteoarthritis during three activities of daily living. Clinical Biomechanics. 2020 Feb; 72: 16–23.
53. Nalband S, Sundar A, Prince AA, Agarwal A. Feature selection and classification methodology for the detection of knee-joint disorders. Computer Methods and Programs in Biomedicine. 2016 Apr; 127: 94–104.
54. Nalband S, Prince A, Agrawal A. Entropy-based feature extraction and classification of vibroarthographic signal using complete ensemble empirical mode decomposition with adaptive noise. IET Science, Measurement & Technology. 2018 May; 12(3): 350–9.
55. Wu Y, Chen P, Luo X, Huang H, Liao L, Yao Y, et al. Quantification of knee vibroarthrographic signal irregularity associated with patellofemoral joint cartilage pathology based on entropy and envelope amplitude measures. Computer Methods and Programs in Biomedicine. 2016 Jul; 130: 1–12.
56. Mascarenhas E, Nalband S, Fredo ARJ, Prince AA. Analysis and Classification of Vibroarthrographic Signals using Tuneable 'Q' Wavelet Transform. In: 2020 7th International Conference on Signal Processing and Integrated Networks (SPIN) [Internet]. Noida, India: IEEE; 2020 [cited 2022 Apr 1]. 65–70. Available from: https://ieeexplore.ieee.org/document/9071335/
57. Sharma M, Acharya UR. Analysis of knee-joint vibroarthographic signals using bandwidth-duration localized three-channel filter bank. Computers & Electrical Engineering. 2018 Nov; 72: 191–202.
58. Nalband S, Valliappan CA, Prince RGAA, Agrawal A. Feature extraction and classification of knee joint disorders using Hilbert Huang transform. In: 2017 14th International Conference on Electrical Engineering/Electronics, Computer, Telecommunications and Information Technology (ECTI-CON) [Internet]. Phuket: IEEE; 2017 [cited 2022 Apr 1]. 266–9. Available from: http://ieeexplore.ieee.org/document/8096224/
59. Wu Y, Cai S, Yang S, Zheng F, Xiang N. Classification of Knee Joint Vibration Signals Using Bivariate Feature Distribution Estimation and Maximal

Posterior Probability Decision Criterion. Entropy. 2013 Apr 17; 15(12): 1375–87.

60. Cai S, Yang S, Zheng F, Lu M, Wu Y, Krishnan S. Knee Joint Vibration Signal Analysis with Matching Pursuit Decomposition and Dynamic Weighted Classifier Fusion. Computational and Mathematical Methods in Medicine. 2013; 2013: 1–11.
61. Mu T, Nandi AK, Rangayyan RM. Screening of knee-joint vibroarthrographic signals using the strict 2-surface proximal classifier and genetic algorithm. Computers in Biology and Medicine. 2008 Oct; 38(10): 1103–11.
62. Zheng Y, Wang Y, Liu J, Jiang H, Yue Q. Knee joint vibration signal classification algorithm based on machine learning. Neural Comput & Applic. 2021 Feb; 33(3): 985–95.
63. Kim KS, Seo JH, Kang JU, Song CG. An enhanced algorithm for knee joint sound classification using feature extraction based on time-frequency analysis. Computer Methods and Programs in Biomedicine. 2009 May; 94(2): 198–206.
64. Balajee A, Murugan R, Venkatesh K. Security-enhanced machine learning model for diagnosis of knee joint disorders using vibroarthrographic signals. Soft Comput. 2023 Jun; 27(11): 7543–53.
65. Rangayyan RM, Wu Y. Analysis of Vibroarthrographic Signals with Features Related to Signal Variability and Radial-Basis Functions. Ann Biomed Eng. 2009 Jan; 37(1): 156–63.
66. Semiz B, Hersek S, Whittingslow DC, Ponder LA, Prahalad S, Inan OT. Using Knee Acoustical Emissions for Sensing Joint Health in Patients With Juvenile Idiopathic Arthritis: A Pilot Study. IEEE Sensors J. 2018 Nov 15; 18(22): 9128–36.